ELSEVIER

Journal of Photochemistry and Photobiology A: Chemistry 152 (2002) 155–165

Journal of Photochemistry and Photobiology A:Chemistry

www.elsevier.com/locate/jphotochem

Synergetic effect in degradation of formic acid using a new photoelectrochemical reactor

Taicheng An [a,*], Ya Xiong [a,*], Guiying Li [b,*], Changhong Zha [a], Xihai Zhu [a]

[a] *School of Chemistry and Chemical Engineering, Zhongshan University, Guangzhou 510275, PR China*
[b] *School of Life Science, Northwest Normal University, Lanzhou 730070, PR China*

Received 19 November 2001; received in revised form 29 March 2002; accepted 15 May 2002

Abstract

Degradation of formic acid was investigated using a novel photoelectrocatalytic reactor with a porous titanium plate as an air distributor as well as an electrode. By the comparison of the COD removal efficiencies from the solution containing formic acid for three processes, direct electro-oxidation, photocatalysis and photoelectrocatalysis, a significant photoelectrochemical synergetic effect was observed in the photoelectrocatalysis process. The synergetic effect was assessed with a new parameter, synergetic factor (SF). The effects of various operating conditions, such as applied cell voltage, treating time, airflow, initial pH value, catalyst amounts and conductivity of solution, on the SF were investigated as well. It was found that the SF was considerably dependent on these operating conditions, moreover, not simply proportional to them.

Keywords: Photoelectrocatalysis; Photocatalysis; Electro-oxidation; Formic acid; Photoelectrochemical reactor; Synergetic effect

1. Introduction

Photoelectrochemical technology with external field appears to be a newly emerging research front of photocatalytic degradation of organic pollutants [1–3]. Many academic interests have been focused on the area in recent year [1–6]. It has been repeatedly confirmed that the external electric field could enhance greatly photocatalytic efficiency, which is well known as an electric field enhancement effect [2,7,8].

However, for any hybrid technology, it is frequently sought that the efficiency of the hybrid system (AB) had better, at least theoretically, be higher than the sum of efficiencies of the two single technologies (A and B) consisting of the hybrid one, that is, AB > A + B. And the experimental phenomenon is considered as an indicator of synergetic effect originated from the interaction between the single technologies [6,9–11].

With respect to the photoelectrochemical technology with external electric field, a hybrid technology combining photocatalytic oxidation with electrochemical oxidation, so far, most of these researches were focused on representing a proof-of-concept that anodic bias on TiO_2 electrode could drive away the photogenerated electron and hole in different directions and reduce their recombination, leading to an increase in photocatalytic efficiency. There is rare publication concerning photoelectrochemical synergetic effect. Pelegrini et al. [6] have once reported an observation of synergetic effect related to the photoelectrochemical degradation of C.I. Reactive Blue 19. They found that the removal efficiencies of both color and TOC from the solution containing C.I. Reactive Blue 19 with a photoelectrochemical technology were higher than the sum of those by a single application of electrochemical and photocatalytic process. However, for all we know, the effect of various operating conditions on synergetic effect in the process of photoelectrochemical degradation of organic pollutants has still not been investigated to date. Our interest in this study was to probe the change law of the photoelectrochemical synergetic effect with operating conditions.

HCOOH was selected frequently as a model organic pollutant in the experiments of photoelectrochemical detoxification of water by many research groups [2,4,8,12–15] because it has no light absorption in the range 320–400 nm, no significant homogeneous photodegradation reactions and no spontaneous evaporation from solution [13]. Furthermore, formic acid not only exists in some actual industrial wastewater such as effluent from tanners, dye workshops, printed fabrics mills

* Corresponding authors. Present address: Guangzhou Institute of Geochemistry, Chinese Academy of Sciences, Guangzhou 510640, China. Tel.: +86-20-85290190; fax: +86-20-85290706.
E-mail address: antc99@gig.ac.cn (T. An).

1010-6030/02/$ – see front matter © 2002 Elsevier Science B.V. All rights reserved.
PII: S1010-6030(02)00211-3

[16], but also is one of stable intermediates, a resistance to further oxidation [17,18], in the complete mineralization of many organic pollutants [19–22]. As a part of our researches, the aim of the present paper is to investigate the effect of various operating conditions, such as applied cell voltage, treating time, airflow, pH value, catalyst amount, and the conductivity of solution, on the synergistic effect in degradation of formic acid using a new photoelectrochemical reactor. The synergetic effect was evaluated using a new-defined parameter, synergetic factor (SF). According to Pelegrini et al.'s researches [6,9–11], in this paper the SF was defined as

$$\mathrm{SF} = R_{\mathrm{pe}} - (R_{\mathrm{p}} + R_{\mathrm{e}}) \quad (1)$$

where R_{pe}, R_{p} and R_{e} are the efficiencies or kinetic constants of COD removal for photoelectrochemical, photocatalytic and electrochemical process, respectively. If $\mathrm{SF} > 0$, the process has a synergetic effect concerning photocatalysis and electrochemistry. And the greater the SF, the stronger the synergetic effect. Conversely, if $\mathrm{SF} \leq 0$, the process has possibly no synergetic effect.

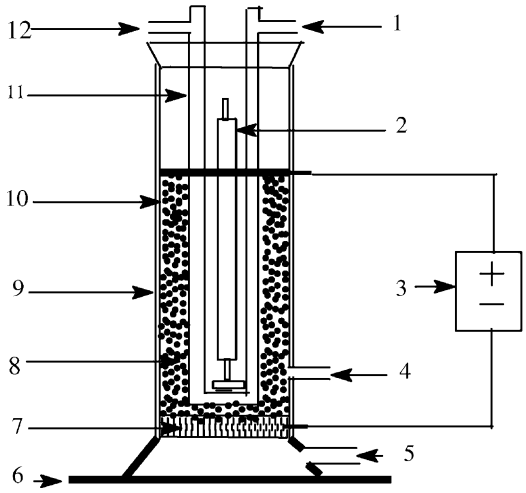

Fig. 1. Schematic of reactor setup—1: inlet of recycled water; 2: high-pressure mercury lamp; 3: CHI650A electrochemical system; 4: sampling outlet; 5: inlet of compressed air; 6: base of reactor; 7: micropore titanium plate and cathode; 8: slurry of TiO_2; 9: aluminum foil; 10: outer Pyrex cylinder; 11: double-welled quartz U-tube; 12: outlet of recycled water.

2. Experimental

2.1. Materials

Photocatalyst was titanium dioxide Degussa P25, mainly anatase (ca. 70%) under the shape of non-porous polyhedral particles of ca. 30 nm mean size with a surface area of $50\,\mathrm{m^2\,g^{-1}}$. Formic acid was analytic grade reagent, and the solutions were prepared with deionized water to the concentration of $20\,\mathrm{mmol\,l^{-1}}$ (COD: 320 ppm). The micropore titanium plate was used as electrodes after disposed with diluted sulfuric acid and then washed with deionized water twice, respectively. All other reagents were analytic grade.

2.2. Apparatus

Absorption spectra of formic acid were recorded with a mode UV-PC2501 spectrophotometer (SHIMASZU, Japan). Current was measured with a computerized CHI650A electrochemical system (Shanghai, China), which was also used as a potentiostat. Scanning electron micrographies were obtained on a HITACHI S520 mode reflection electronic microscope.

2.3. Photoelectrochemical reactor

The used setup is a batch slurry photoelectrochemical reactor. As shown in Fig. 1, it consisted of an outer cylindrical Pyrex casing (i.d. = 55 mm; height = 250 mm) fitted with a gas distributor (porous titanium plate with a pore size of less than 40 μm) and a PVC base. A 500 W high-pressure mercury lamp suspended vertically in a double-welled U-tube through which a 5.0 mm thick cooling water flows ($650\,\mathrm{ml\,min^{-1}}$) to maintain reaction isothermality. The circulating water also ensured infrared filtering of the incident ray [10]. The slurry solution containing Titania particles was placed between the annulus of the quartz U-tube and the outer Pyrex cylinder and the thickness of the slurry solution is 5.0 mm. The compressed air was bubbled upwards through the porous titanium plate as a gas distributor equipped with the bottom of reactor. Simultaneously, the titanium gas distributor was also used as the cathode of the photoelectrochemical reactor while its anode is a cirque made of porous titanium, located above the cathode about 15 cm distant. Additionally, the exterior wall of the reactor was covered with a reflecting aluminum foil, similar to the photoreactor which Haarstrick et al. [23] reported.

2.4. Analysis

Millipore Disks (0.45 μm) was used to remove particulate mass of the colloid solution before the COD analysis, and the COD was measured with potassium dichromate.

2.5. Recommended procedure

A 200.0 ml solution of formic acid containing titanium dioxide was fed into the photoelectrochemical reactor each run. The reactor was timed starting when the d.c. power, illumination and compressed air supply were switched on. Except as indicated, general treating conditions were 10.0 V voltage, $0.1\,\mathrm{m^3\,h^{-1}}$ airflow, 0.02 g titanium dioxide, 2.5 pH value, $0.757\,\mathrm{mS\,cm^{-1}}$ conductivity, and 60 min treatment time. The resulting colloid solutions were separated with centrifuge and then filtered through a Millipore (0.45 μm) membrane for optical absorption and COD analysis.

3. Results and discussion

3.1. Characterization of photoelectrochemical reactor

3.1.1. Micrographic characterization

It is well known that molecular oxygen plays an important role in the photocatalytic reaction. The oxygen was frequently used to capture the photogenerated electrons [24] in a lots of photocatalytic experiments. Although the use of external electric field obviates the need of oxygen as an electron acceptor in the photoelectrochemical reaction, the presence of molecular oxygen affects both the rate and degradation pathways of organic pollutants [25,26]. Furthermore, in general, a bubble column reactor with porous plate distributor can offer best gas–liquid mass transfer efficiency [27]. In the view of above considerations, a kind of special porous titanium plate was used as a gas distributor in this study. The SEM micrographs of the surface and section of the porous titanium plate are presented in Fig. 2. The SEM micrographs show that the plate is rather regular and porous. It can been seen from Fig. 3 that many fine distributed air bubbles with a size of about 1 mm generated in the reactor, are beneficial to mass transfer and oxygen dissolving. It is worth mention that the porous titanium plate was used not only as a distributor but also as a cathode in this reactor, differing from all reported photoelectrochemical reactors.

3.1.2. Current–voltage characteristics

The application of external electric field provides a potential gradient to drive away the photogenerated holes and electrons in different directions efficiently. Thus the external electric field can minimize charge recombination. The current–voltage behavior reflects directly the competition between hole-mediated and electron-consumed reactions [28]. Thus, the magnitude of the photocurrent is one of the major parameters characterizing photoelectrochemical reactor. The photocurrent was extensively investigated in the slurry and thin film photoelectrochemical reactors [25,28–33].

In the present reactor, the changes in the current of photoelectrocatalytic as well as electrochemical processes with cell voltage were also measured in the presence of 20 mmol l^{-1} formic acid. The obtained current–voltage profiles are shown in Fig. 4. Seen from the figure, both current of photoelectrochemical and electrochemical processes increased significantly with increase in the applied voltage. But the former is always higher than the latter, even the sum of the latter and photocurrent (34.3 μA, current in the absent of applied voltage), being a clear evidence of the synergetic effect between photochemical and electrochemical process. Simultaneously, it is also observed from the figure that when the cell voltage lower than 5 V, the SF increases as the increase of cell voltage. But, over 5 V, SF did not change almost. This result suggested that in the range 0–5 V, the high the applied voltage, the stronger the ability

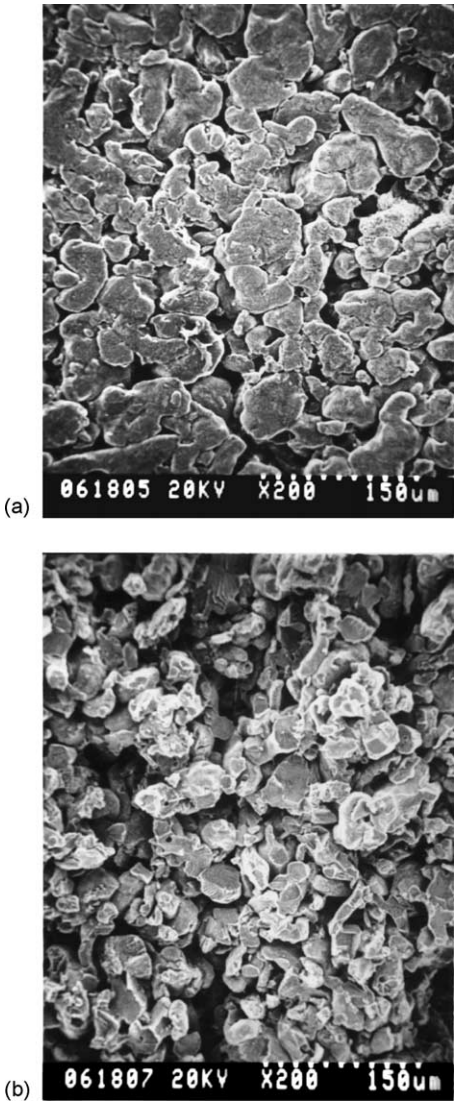

Fig. 2. SEM image of micropore titanium plate. (A) surface; (B) section.

of capturing photogenerated electron by external electric field. However, as for the reason why the SF remains constant when the cell voltage higher than 5 V. At the present time, we do not know how to explain this observation well. The additional experimental must be conducted to clarify the reason in the further paper.

The current–time curves for photoelectrocatalytic process was also measured at the presence of 20 mmol l^{-1} formic acid in the solution. As shown in Fig. 5, the curves at various applied voltages all decrease continuously with time. This means that the current decrease as formic acid is degraded in the solution. The observation is similar to the result reported by Candal et al. [34], although the used slurry reactor in this study is different from their reactor, a thin film reactor. Furthermore, the current decrease much faster at the cell voltage of 10.0 than 1.0 V. This denotes that the higher the cell voltage, the faster the degradation of formic acid.

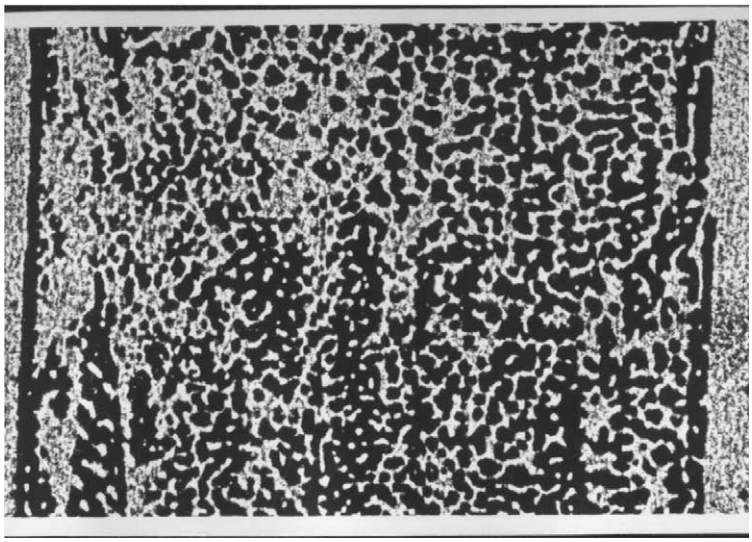

Fig. 3. Photograph of air bubble in the photoelectrocatalytic reactor.

3.2. Effect of various factors on synergistic effect

3.2.1. Effect of applied cell voltage

The effect of applied voltage on COD removal in photoelectrochemical process was conducted and the profile is shown in the inset of Fig. 6. In the profile, it is obvious that the COD removal efficiency increase in the range of less than 5 V, then no more change with the increase of applied voltage over 5 V, leading to a well-defined flat with a COD removal enhancement of ca. 35.6% compared with photocatalytic process at the absence of voltage (62.9%). Therefore, the experimental result indicates that external electric field can control conveniently the performance of photocatalytic reaction in the new-designed slurry reactor. This conclusion seems not to conform to Vinodgopal et al.'s view [35] because that they believed that it was not possible to influence a photoreaction in a TiO_2 slurry system with an externally applied potential bias. The insert of Fig. 6 also shows the dependence of COD removal on the applied voltage in an electrochemical process. The COD removal also increase slightly with increase in applied voltage, but the increase is much less than that in current with the applied voltage as shown in Fig. 4. This is possible due to that the parasitic reactions, such as O_2 and H_2 generation, consume much current.

The dependence of SF on applied voltage is presented in Fig. 6. It can be seen from the figure that in the range

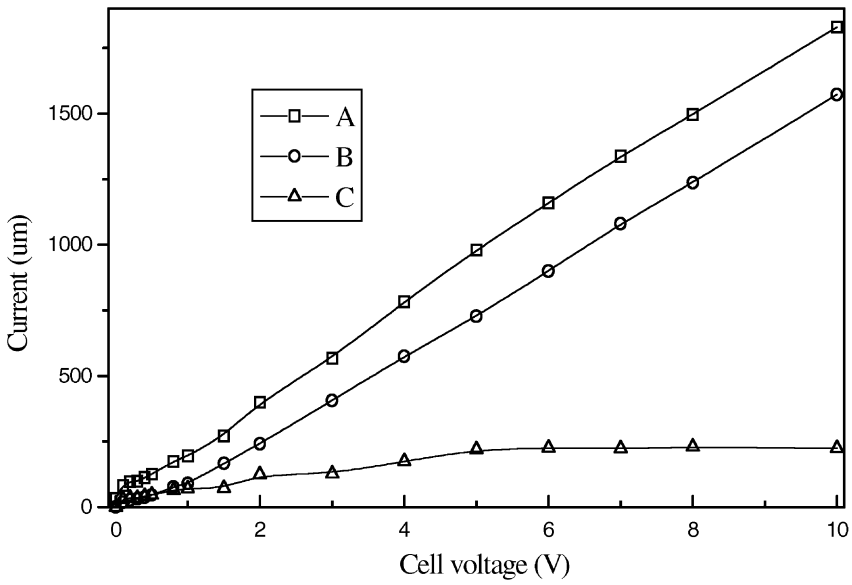

Fig. 4. Current–voltage characteristics. A: The current at initial 10 s in the photoelectrochemical process; B: the current at initial 10 s in the electrochemical process; C: synergetic factor.

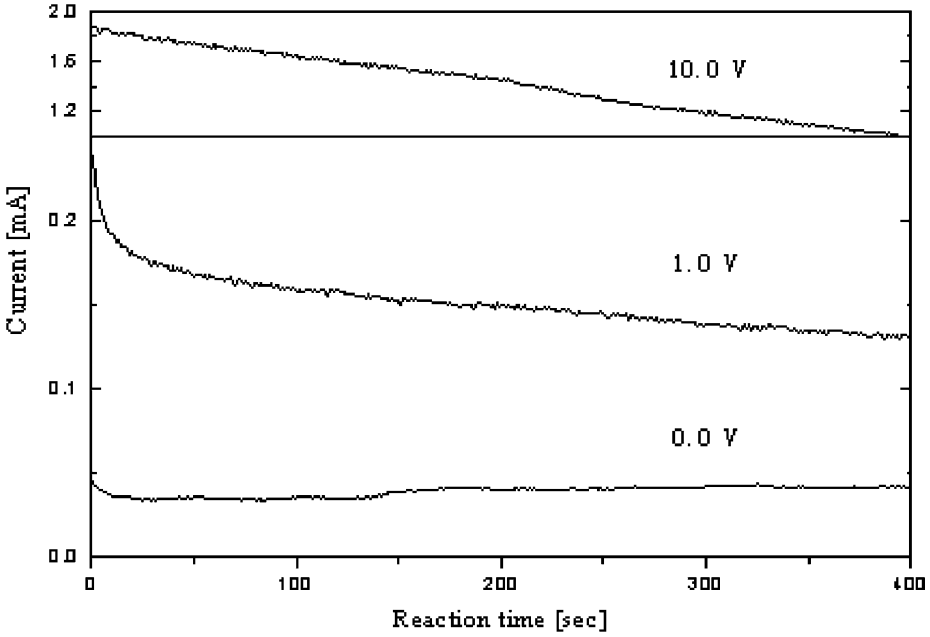

Fig. 5. Effect of reaction time on photocurrent change.

of the tested voltage, all SFs are greater than 0. And SF increases first with increasing in voltage, then reaches a maximum value, 31.6%, at about 5 V. The observations denote that there is a significant synergistic effect existing in the photoelectrochemical process. And the higher the applied voltage, the stronger the synergistic effect, at least in the range 0–5 V. The synergistic effect may be due to that the higher the applied voltage, the stronger the ability of capturing photogenerated electron by the electric field, leading to more efficiently reducing the recombination of photogenerated electron and hole.

3.2.2. *Effect of airflow*

During the experiment, the compressed air was sparged into the reactor from the bottom of the reactor through porous titanium plate. As mentioned previously, the sparged air can not only speed up mass transfer but also increase the dissolving of oxygen. As a result, it is expected that the sparged compressed air will play an important role in the photoelectrochemical synergically degradation of formic acid.

The inset of Fig. 7 shows that COD removal efficiencies increase considerably with increase in airflow for both

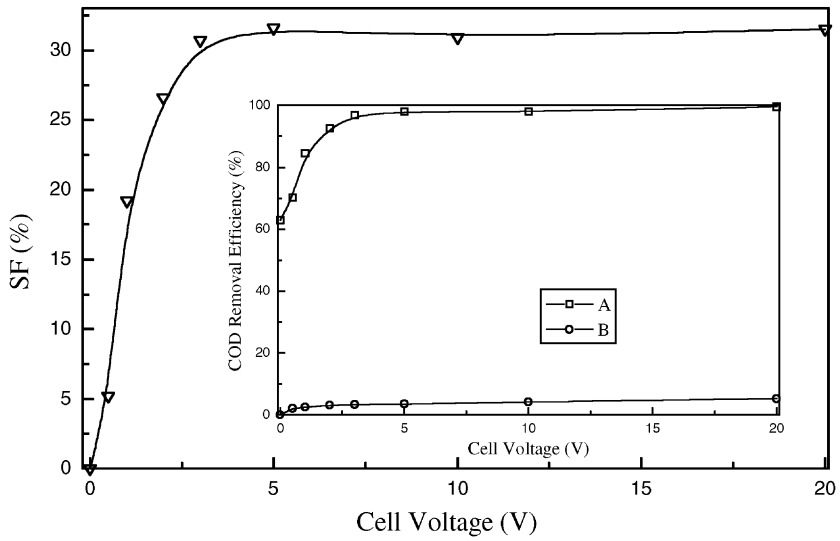

Fig. 6. Effect of applied cell voltage. A: Photoelectrocatalysis; B: electro-oxidation.

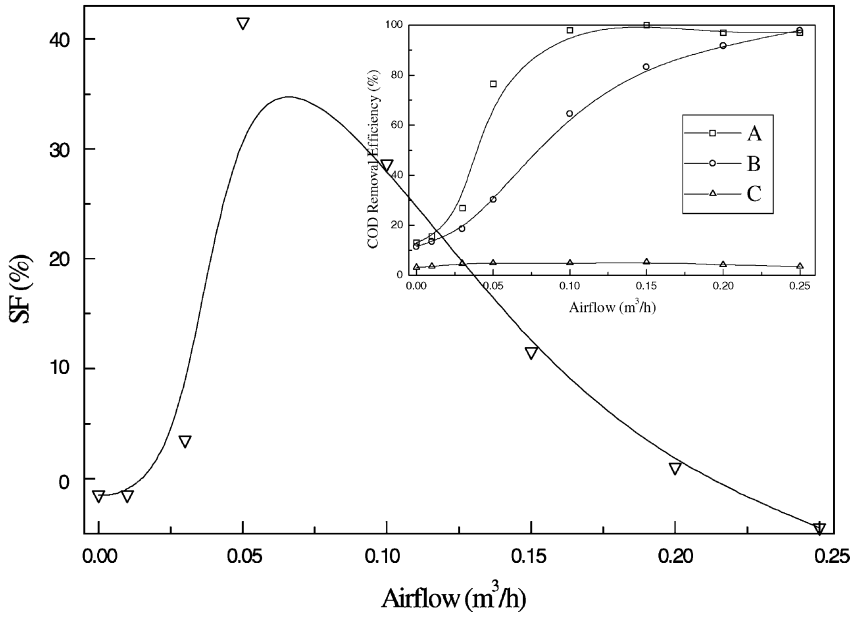

Fig. 7. Effect of airflow. A: Photoelectrocatalysis; B: photocatalysis; C: electro-oxidation.

photocatalytic and photoelectrocatalytic processes, in spite of only slight increase for electrochemical process. These are due to the enhancement effect in mass transfer and capture agent of photogenerated electron, dissolved oxygen. Simultaneously, it can still be seen from Fig. 7 that photoelectrochemical synergetic effect also increase obviously with increase in airflow, at least, in the range of less than about $0.07\,m^3\,h^{-1}$. This observation can be interpreted in the term of the effect of mass transfer. The sparged air can efficiently enhance the collision of photoexcited TiO_2 particle in slurry with the surface of electrode, which makes electric field more facilitate to capture photogenerated electrons. As for decrease in SF over about $0.07\,m^3\,h^{-1}$ airflow, a probable reason is that the COD removal efficiency has approached 100%, no possibility to increase further after about $0.07\,m^3\,h^{-1}$ airflow for photoelectrocatalytic process, while the COD removal efficiency do not reach a limited value and increase continuously for photocatalytic process. Therefore, the SF and the difference between the COD removal efficiencies for the two processes decrease.

3.2.3. *Effect of photocatalyst amount*

In every photoreactor used, the optimal concentration of titanium dioxide has to be determined since it strongly dependents on the geometry of the photoreactors and the incident flux as well on the mean optical pathway within the suspension [36]. Lea and Adesina [27] found that the photocatalytic rate increased at low catalyst loading, but dropped after loading levels higher than $1\,g\,l^{-1}$. More recently, Assabane et al. [36] also investigated this subject. They observed that the rate curve first increased, then leveled off. No decrease of rate was found.

Presently, the influence of TiO_2 concentration on COD removal is studied from 0 to $0.75\,g\,l^{-1}$ not only for photocatalytic process but also for electrochemical and photoelectrochemical processes. As shown in the inset of Fig. 8, the COD removal of electrochemical process changes slightly with TiO_2 concentration. However, the curve of COD removal of either photoelectrochemical or photocatalytic process first increase substantially with the increase in the concentration of TiO_2 and then level off beyond $0.1\,g\,l^{-1}$ for the former. But curve continues to gradually rise for the latter when TiO_2 concentration is less than $0.75\,g\,l^{-1}$. The change of photocatalytic process is similar to that reported by Assabane et al. [36]. It is worth notice that the optimum TiO_2 concentration of photoelectrocatalytic process corresponds to $0.1\,g\,l^{-1}$, that is, a 10 times smaller value than that reported in photocatalytic reactor [36].

The change of SF with TiO_2 concentration is presented in Fig. 8. It is manifested from the figure that SF increases first, then gradually falls, appearing a maximum value at $0.3\,g\,l^{-1}$ TiO_2. The increase in SF at low catalyst concentration indicated that the synergetic effect is approximately proportional to the total number of active sites. At high TiO_2 concentration, there is a additional unfavorable factor, loss in surface area available for light-harvesting caused by the agglomeration effect of external electric field for photoelectrocatalytic process, in addition to light scattering and shielding as the number of particles in solution increased as that observed in photocatatlytic process [36]. The decrease in SF at high catalyst concentration can be attributed to the agglomeration effect of the external electric field. The effect increases an additional complication involved in the design of photoelectrochemical reactor compared with photocatalytic reactor.

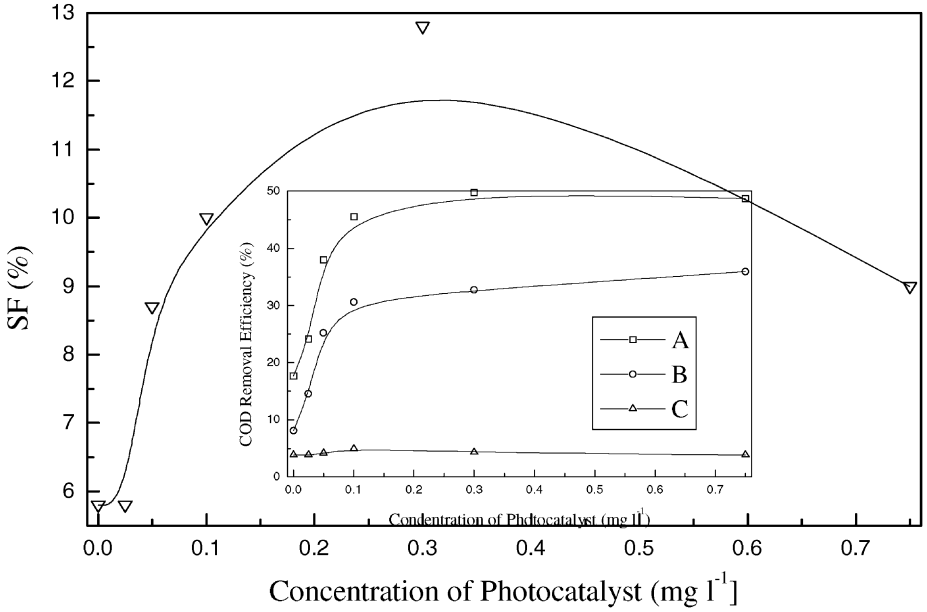

Fig. 8. Effect of photocatalyst concentration (treating time: 30 min). A: Photoelectrocatalysis; B: photocatalysis; C: electro-oxidation.

3.2.4. *Effect of treatment time*

The UV spectra of formic acid in the photoelectrochemical process at various reaction intervals are presented in Fig. 9. It can be observed from the figure that formic acid decreased dramatically. And the COD removal efficiencies, at any tested time, are much higher than that for either photocatalytic or electrochemical process as shown in Fig. 10, resulting in that SF is always greater than 0. Furthermore, it is found from Fig. 10 that the SF increased greatly before 50 min, then decreased significantly after the time. This phenomenon can be simply understood that the longer the reaction time, the more the captured photogenerated electrons, thus the synergetic effect is more apparent. Nevertheless, after 50 min, the COD removal efficiency for the photoelectrochemical reaction is closed to 100%, a limited value, while the COD removal efficiency for either photocatalytic or electrochemical process is keeping increasing so that the SF begins to drop.

It is also well recognized that photocatalytic degradation of organic pollutants accords with pseudo first-order kinetics [10,37–40]. In this work, pseudo first-order kinetics were also confirmed not only in the photocatalytic but also in the

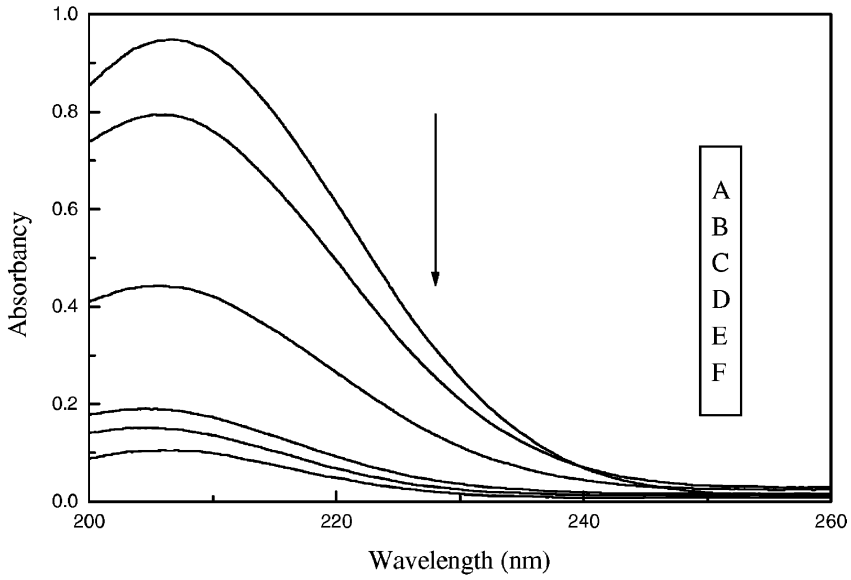

Fig. 9. U-spectra change of formic acid. A: 0 min; B: 10 min; C: 20 min; D: 30 min; E: 40 min; F: 60 min.

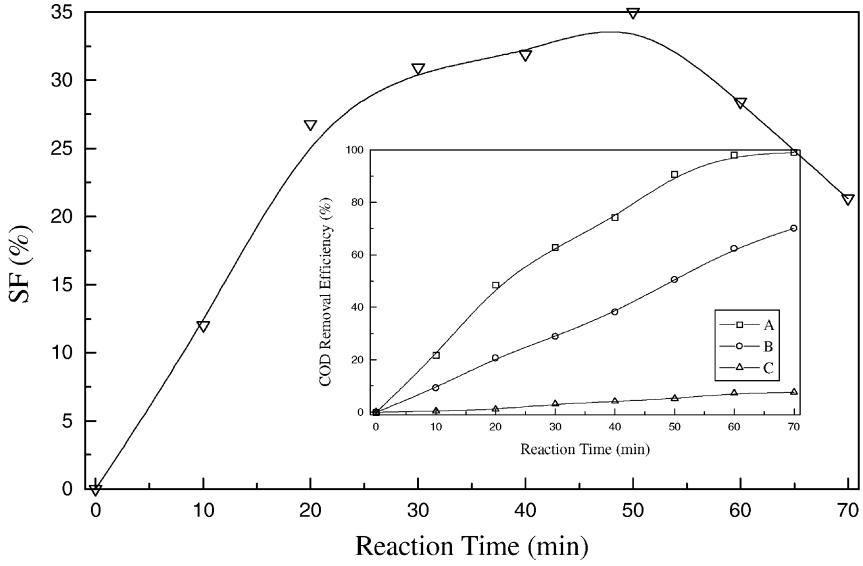

Fig. 10. Effect of treatment time. A: Photoelectrocatalysis; B: photocatalysis; C: electro-oxidation.

electrochemical as well as in the photoelectrocatalytic process by the linear transforms $\ln(COD_0/COD_t) = f(t)$ of Fig. 10 as shown in Fig. 11. The kinetic regression equations and parameters were listed in Table 1, respectively. The SF obtained from the kinetic constant is 0.0274 min^{-1}, revealing further that an apparent synergetic effect exists in the photoelectrocatalytic process.

3.2.5. *Effect of initial pH value*

pH value is an important parameter in the photocatalytic and photoelectrocatalytic degradation of formic acid. One is due to that the iso-electric point of TiO_2 is at pH between 4 and 6 [14]. Hence, at more acidic pH values, the catalyst surface is positively charged while at pH value above 6, it is negatively charged. The other is due to that formic acid is a kind of weak organic acid. Its existing forms are dependent on pH value of solution. HCOOH is a main form at low pH value, while $HCOO^-$ is a main form at high pH. Therefore, the pH value will have significant effect on the adsorption–desorption properties of formic acid at the catalyst's surface.

Kim and Anderson [14,34] have successfully investigated the effect of pH on the photoelectrocatalytic and photocatalytic degradation of formic acid. However, it is expected

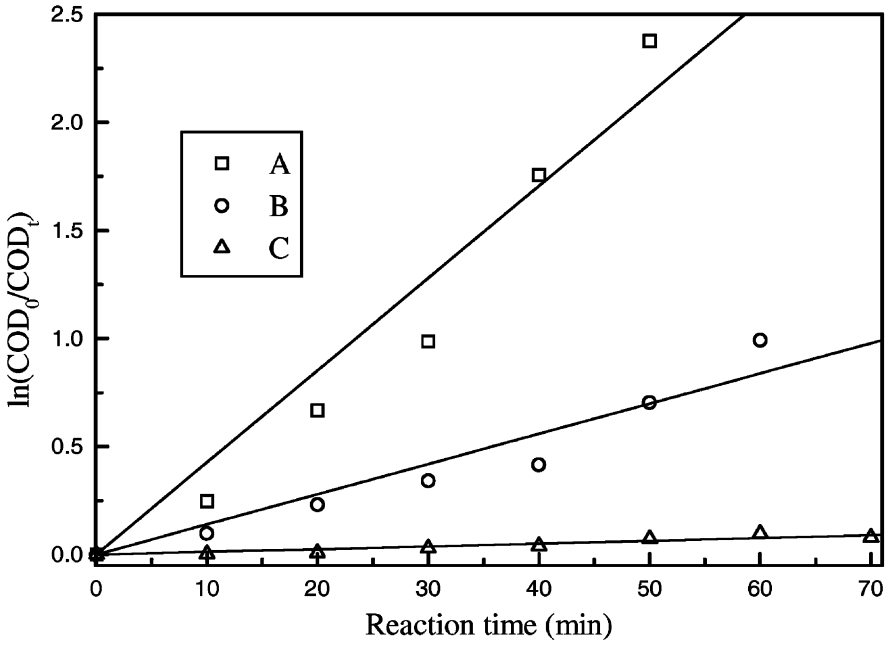

Fig. 11. Kinetic curves of various process. A: Photoelectrocatalysis; B: photocatalysis; C: electro-oxidation.

Table 1
Kinetic equations and parameters of formic acid in various conditions

Systems	PEC	PC	EC
Regression equation	$Y = 0.0427t$	$Y = 0.0140t$	$Y = 0.0013t$
Regression coefficiency	0.9822	0.9698	0.9507
Apparent rate constant K (min^{-1})	0.0427	0.0140	0.0013
Half-life (min)	16.2	49.5	533.2
SF (min^{-1})	0.0274		

that pH value of solution possibly also affect the synergistic effect as photoelectrochemical and photocatalytic reaction. Herewith we attempt to probe further the point.

The experimental results in the pH range 1.5–10.5 are shown in the inset of Fig. 12. The COD removal efficiencies are significantly affected by the changes of the pH value of solution, and the maximum removal efficiencies were obtained at approximately pH 3.5 with respect to the photoelectrocatalytic and photocatalytic processes, above or below this pH value, both curves dropped. The results are similar to that reported by Kim and Anderson [14,34] although the slurry reactor used in this experiment is rather different from their reactor, a TiO_2 thin films reactor. But a slight discrepancy was also observed at basic solution. At pH 6.0, a COD removal efficiency of ca. 58% were obtained in the photoelectrocatalytic process while no degradation was detected over this pH value in their experiment.

The dependence of SF on the initial pH value is also shown in Fig. 12. It can be seen that SF decrease greatly and approached to a minimum at ca. pH 3.5 and thereafter increase rapidly. At this moment, it is not clear why synergetic effect is minimum at pH 3.5, that is, an optimal pH value, while SF is greater above or below this pH value. The complete understanding to the issue needs to wait for further researches.

3.2.6. *Effect of conductivity*

In this study, Na_2SO_4 was selected as an electrolyte for controlling the conductivity of formic acid solution. Fig. 13 shows that the change curves of the COD removal efficiencies with the conductivity in the electrochemical, photocatalytic and photoelectrocatalytic processes, respectively. The COD removal efficiency for the photocatalytic process significantly dropped while increasing in the conductivity of solution, due to the competition adsorption between SO_4^{2-} and formate at the TiO_2 surface. The result is consistent with that reported by Kim et al. [13] and Burns et al. [41] rather than Zhu et al. [42]. Compared with the photocatalytic process, the photoelectrocatalytic process displayed a more complex change tendency of COD removal efficiency with the conductivity. As shown in Fig. 13, the COD removal first drops then increases with increase in the conductivity. The above observations can be interpreted as follows. The decrease at low conductivity can be attributed to the competition adsorption between SO_4^{2-} and formate at the TiO_2 surface. At high conductivity, the adsorption of SO_4^{2-} reaches equilibrium, the surplus free SO_4^{2-} as an electrolyte can enhance charge transfer in the slurry reactor, leading to increase in efficiency of direct electrochemical oxidation, as revealed in the curve C of Fig. 13, and in capture of photogenerated electron by external electric field.

Additionally, it was noticed that the COD removal efficiency corresponding to the greatest conductivity, 2.85 mS cm^{-1}, in the experiment is still ca. 25%, less than that without additional SO_4^{2-}. The decreased value is rather

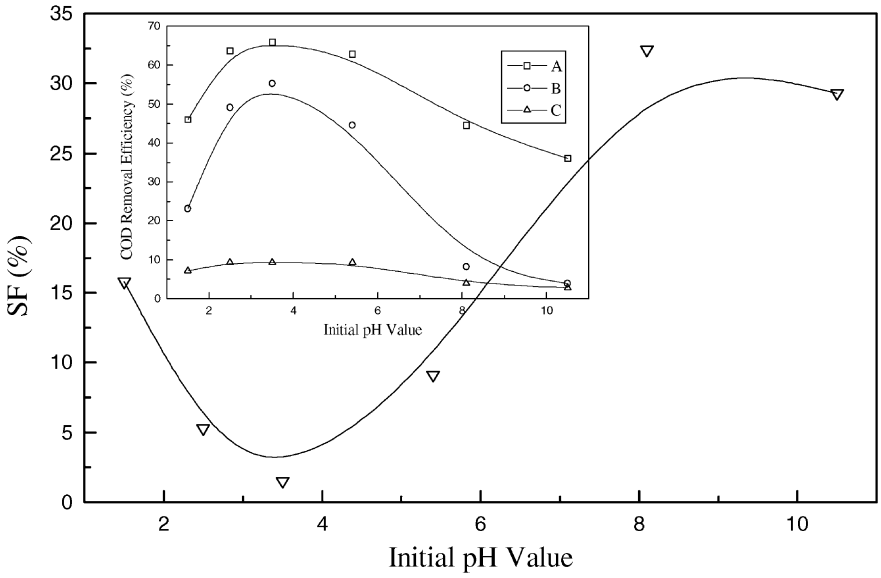

Fig. 12. Effect of initial pH value. A: Photoelectrocatalysis; B: photocatalysis; C: electro-oxidation.

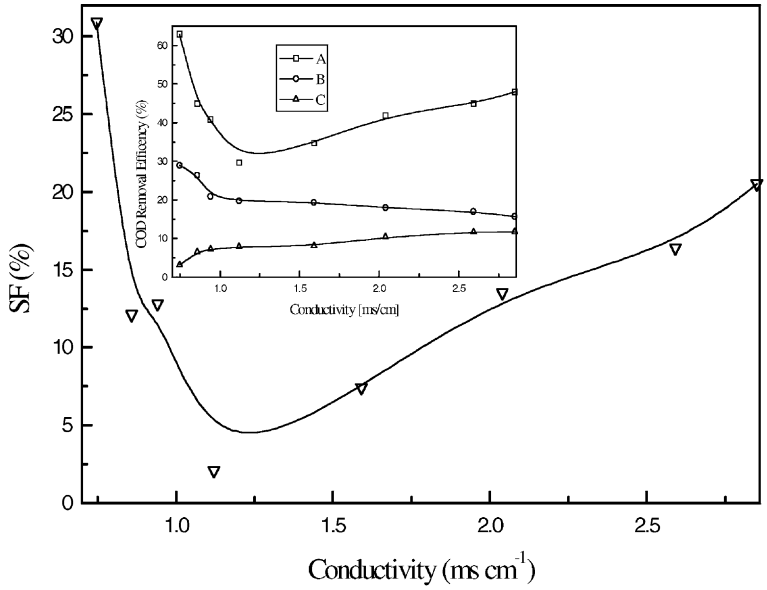

Fig. 13. Effect of conductivity (treating time: 30 min). A: Photoelectrocatalysis; B: photocatalysis; C: electro-oxidation.

closed to that reported by Kim et al. [13] (ca. 21%, calculating with the data in their Fig. 7). Therefore, the addition of Na_2SO_4 is unfavorable to either the photocatalytic and photoelectrocatalytic reactions.

The dependence of SF on conductivity is also presented in Fig. 13. Its change tendency is similar to that of curve A of Fig. 13. The increase of SF with conductivity at high SO_4^{2-} concentration further suggests that free SO_4^{2-} may enhance photogenerated electron transfer in the slurry solution, leading to an increase in the synergetic effect.

4. Conclusion

The primary study revealed that the synergetic effect was considerably dependent on various operating conditions, such as applied cell voltage, treating time, airflow, pH value, catalyst amount, and the conductivity of solution. Moreover, it was not simple proportional to these operating conditions. The additional experiments related to the synergetic effect are in progress in order to probe further its change law and to clarify further the reason for the change at other conditions and/or other systems.

Acknowledgements

This work was supported by the NSF of China (29977030), Sci. & Technol. Project of Guangdong (20010670A), NSF of Guangdong Province (990274), Sci. & Technol. Project of Guangdong EPA (1999-14), and State Key Laboratory of Organic Geochemistry, Guangzhou Institute of Geochemistry, China Academy of Sciences.

References

[1] A.J. Bard, Science 207 (1980) 139–144.
[2] I.M. Butterfield, P.A. Christensen, A. Hamnett, K.E. Shaw, G.M. Walker, S.A. Walker, C.R. Howarth, J. Appl. Electrochem. 27 (1997) 385–395.
[3] J.A. Byrne, B.R. Eggins, W. Byers, N.M.D. Brown, Appl. Catal. B 20 (1999) L85–L89.
[4] R.J. Candal, W.A. Zeltner, M.A. Anderson, J. Adv. Oxid. Technol. 3 (1998) 270–276.
[5] J.A. Byrne, B.R.J. Eggins, Electroanal. Chem. 457 (1998) 61–72.
[6] R. Pelegrini, P. Perqlta-Zamora, A.R. Andrade, Appl. Catal. B 22 (1999) 83–90.
[7] K. Vinodgopal, S. Hotchandani, P.V. Kamat, J. Phys. Chem. 97 (1993) 9040–9044.
[8] J.M. Kesselman, N.S. Lewis, M.R. Hoffmann, Environ. Sci. Technol. 31 (1997) 2298–2302.
[9] J.M. Herrmann, J. Matos, J. Disdier, C. Guillard, J. Laine, S. Malato, J. Blanco, Catal. Today 54 (1999) 255–265.
[10] J. Matos, J. Laine, J.M. Herrmann, Appl. Catal. B 18 (1998) 281–291.
[11] J. Matos, J. Laine, J.M. Herrmann, Carbon 37 (1999) 1870–1872.
[12] S. Hyun, K. Lee, Memburein 6 (1996) 101–108.
[13] D.H. Kim, M.A. Anderson, Environ. Sci. Technol. 28 (1994) 479–483.
[14] D.H. Kim, M.A. Anderson, J. Photochem. Photobiol. A 94 (1996) 221–229.
[15] H. Hidaka, Y. Asai, J. Zhao, K. Nohara, E. Pelizzetti, N. Serpone, J. Phys. Chem. 99 (1995) 8244–8248.
[16] R.J. Candal, W.A. Zeltner, M.A. Anderson, J. Adv. Oxid. Technol. 3 (1998) 270–276.
[17] Y. Ogata, K. Tomizawa, K. Takagi, Can. J. Chem. 59 (1981) 14–18.
[18] J.M. Harmsen, L. Jelemensky, P.J.M. Van, B.F.M. Kuster, G.B. Marin, Appl. Catal. A 165 (1997) 499–509.
[19] S. Chou, Y.H. Huang, S.N. Lee, G.H. Huang, C. Huang, Water Res. 33 (1998) 751–759.
[20] A.P. Davis, D.L. Green, Environ. Sci. Technol. 33 (1999) 609–617.
[21] D.S. Hwang, E.H. Lee, K.W. Kim, K.I. Lee, J.H. Park, J.H. Yoo, S.J. Park, J. Ind. Eng. Chem. 5 (1999) 45–51.

[22] R.M. Dinsdale, F.R. Hwkes, D.L. Hawkes, Water Res. 34 (2000) 2433–2438.
[23] A. Haarstrick, O.M. Kut, E. Heinzle, Environ. Sci. Technol. 30 (1996) 817–824.
[24] G.H. Hung, B.J. Marinas, Environ. Sci. Technol. 31 (1997) 562–568.
[25] K. Vinodgopal, U. Stafford, K.A. Gray, P.V. Kamat, J. Phys. Chem. 98 (1994) 6797–6803.
[26] K. Vinodgopal, P.V. Kamat, CHEMTECH 26 (1996) 18–22.
[27] J. Lea, A.A. Adesina, J. Photochem. Photobiol. A 118 (1998) 111–122.
[28] A. Wahl, M. Ulmann, A. Carroy, J. Augustynski, J. Chem. Soc., Chem. Commun. (1994) 2277–2278.
[29] M.W. Peterson, J.A. Turner, A.J. Nozik, J. Phys. Chem. 95 (1991) 221–225.
[30] A.J. Bard, J. Photochem. 10 (1979) 59–75.
[31] S.A. Walker, P.A. Christensen, K.E. Shaw, G.M. Walker, J. Electroanal. Chem. 393 (1995) 137–140.
[32] A. Wahl, M. Ulmann, A. Carroy, B. Jermann, M. Dolata, P. Kedzierzawski, C. Chatelain, A.A. Monnier, J. Electroanal. Chem. 396 (1995) 41–51.
[33] T. Yoko, A. Yuasa, K. Kamiya, S. Sakka, J. Electrochem. Soc. 138 (1991) 2279–2285.
[34] R.J. Candal, W.A. Zeltner, M.A. Anderson, Environ. Sci. Technol. 34 (2000) 3443–3451.
[35] K. Vinodgopal, S. Hotchandani, V. Kamat, J. Phys. Chem. 97 (1993) 9040–9044.
[36] A. Assabane, Y.A. Ichou, H. Tachiri, C. Guillard, J.M. Herrmann, Appl. Catal. B 24 (2000) 71–80.
[37] R.W. Matthews, Water Res. 25 (1991) 1169–1176.
[38] T.C. An, X.H. Zhu, Y. Xiong, J. Environ. Sci. Health A 36 (2001) 2069–2082.
[39] T.C. An, Y.F. He, Y.J. Fang, X.L. Jin, H. Chen, J. Mol. Catal. A 159 (2000) 143–151.
[40] T.C. An, X.H. Zhu, Y. Xiong, Chemosphere 46 (2002) 897–903.
[41] R.A. Burns, J.C. Crittenden, D.W. Hand, V.H. Selzer, L.L. Sutter, S.R. Salman, J. Environ. Eng. 125 (1999) 77–85.
[42] H. Zhu, M. Zhang, Z. Xia, G.K.C. Low, Water Res. 29 (1995) 2681–2688.